AGU PUBLICATIONS

Geophysical Research Letters

RESEARCH LETTER
10.1002/2016GL068330

Key Points:
- Stratospheric dynamics is crucial for Arctic sea ice and midlatitude climate linkage
- Reduced stratospheric wave mean flow interaction much alters the sea ice impacts on the surface
- Representation of the whole stratosphere is indispensable for realistic climate predictions

Supporting Information:
- Supporting Information S1

Correspondence to:
T. Nakamura,
nakamura.tetsu@ees.hokudai.ac.jp

Citation:
Nakamura, T., K. Yamazaki, K. Iwamoto, M. Honda, Y. Miyoshi, Y. Ogawa, Y. Tomikawa, and J. Ukita (2016), The stratospheric pathway for Arctic impacts on midlatitude climate, *Geophys. Res. Lett.*, *43*, 3494–3501, doi:10.1002/2016GL068330.

Received 17 FEB 2016
Accepted 15 MAR 2016
Accepted article online 21 MAR 2016
Published online 2 APR 2016

The stratospheric pathway for Arctic impacts on midlatitude climate

Tetsu Nakamura[1,2], Koji Yamazaki[1,2], Katsushi Iwamoto[3], Meiji Honda[4], Yasunobu Miyoshi[5], Yasunobu Ogawa[6,7], Yoshihiro Tomikawa[6,7], and Jinro Ukita[4]

[1]Arctic Environmental Research Center, National Institute of Polar Research, Tokyo, Japan, [2]Faculty of Environmental Earth Science, Hokkaido University, Hokkaido, Japan, [3]Mombetsu City Government, Hokkaido, Japan, [4]Department of Environmental Science, Niigata University, Niigata, Japan, [5]Department of Earth and Planetary Sciences, Kyushu University, Fukuoka, Japan, [6]Space and Upper Atmospheric Sciences Group, National Institute of Polar Research, Tokyo, Japan, [7]School of Multidisciplinary Sciences, SOKENDAI (Graduate University for Advanced Studies), Tokyo, Japan

Abstract Recent evidence from both observations and model simulations suggests that an Arctic sea ice reduction tends to cause a negative Arctic Oscillation (AO) phase with severe winter weather in the Northern Hemisphere, which is often preceded by weakening of the stratospheric polar vortex. Although this evidence hints at a stratospheric involvement in the Arctic-midlatitude climate linkage, the exact role of the stratosphere remains elusive. Here we show that tropospheric AO response to the Arctic sea ice reduction largely disappears when suppressing the stratospheric wave mean flow interactions in numerical experiments. The results confirm a crucial role of the stratosphere in the sea ice impacts on the midlatitudes by coupling between the stratospheric polar vortex and planetary-scale waves. Those results and consistency with observation-based evidence suggest that a recent Arctic sea ice loss is linked to midlatitudes extreme weather events associated with the negative AO phase.

1. Introduction

In the global climate system the atmosphere has an important role in connecting climates of different regions, a phenomenon called atmospheric teleconnection, in response to a range of surface boundary conditions. Thus, in investigations of intraseasonal to seasonal climate links between the Arctic and the midlatitudes, it is essential to ask if and how an observed Arctic sea ice loss, by affecting atmospheric circulation aloft, is able to influence weather and climate in remote regions [*Deser et al.,* 2010]. Both observations and numerical simulations have shown that a reduction in the Arctic summer-to-fall sea ice extent, particularly over the Barents-Kara Sea, modulates atmospheric circulation in the subsequent fall-to-winter so as to strengthen the Siberia High, which often brings severe winters to eastern Eurasia [*Honda et al.,* 2009; *Overland et al.,* 2011; *Hopsch et al.*, 2012; *Orsolini et al.,* 2012; *Mori et al.,* 2014]. In addition, when the sea ice cover is low, Northern Hemisphere jets tend to meander, and this meandering often brings anomalously cold weather to the midlatitudes, especially in the Euro-Atlantic sector although there is a debate on this notion especially in terms of the choice of a metric [*Francis and Vavrus,* 2012; *Barnes,* 2013; *Screen and Simmonds,* 2014]. Anomalously, cold winters and meandering jets occur more frequently during the negative phase of the Arctic Oscillation (AO) [*Thompson and Wallace,* 2001; *Barriopedro and Garcia-Herrera,* 2006; *Vavrus et al.,* 2006], which is the predominant variability pattern of the Northern Hemisphere winter climate [*Thompson and Wallace,* 1998]. Dynamically, the negative AO phase represents the atmospheric state in which a larger air mass resides over the polar region and is associated with weak westerlies, anomalously meandering jets in the upper troposphere, and anomalous surface weather patterns.

Recent observational studies have reported that following a summer with a low Arctic sea ice cover, upward propagation of planetary-scale waves is enhanced in late fall and early winter, which leads to a weakened stratospheric polar vortex and subsequent surface signals [*Jaiser et al.,* 2012; *King et al.,* 2015]. On the other hand, modeling studies have also provided supporting evidence for this dynamical process in the stratosphere and troposphere as responses to changes in both sea ice [*Orsolini et al.,* 2012; *Kim et al.,* 2014; *Nakamura et al.,* 2015] and snow boundary conditions [*Fletcher et al.,* 2007; *Peings et al.,* 2012]. Other modeling studies have contradicting results on the AO phase as an Arctic sea ice response [*Cai et al.,* 2012].

At present the exact role of the stratospheric processes in the Arctic-midlatitude climate linkage under the present climatic conditions, especially that associated with an observed rapid sea ice loss, remains unclear. Observationally, it is very difficult to assess the impact of sea ice or snow alone because they might covary

Table 1. Outline of Experiments[a]

Experiment	Run	Integration Period (Years)	Zonal Mean Zonal Wind Restoration	SST	SIT
FREE	*HICE*	60	N/A	*Early*	*Early*
	LICE				*Late*
RS10	*HICE*	60	Above 10 hPa	*Early*	*Early*
	LICE				*Late*
RS30	*HICE*	60	Above 30 hPa	*Early*	*Early*
	LICE				*Late*

[a]*Early* (1979–1983) and *Late* (2005–2009) are the time periods for which monthly average sea surface temperature (SST) or sea ice thickness (SIT) was used for the boundary conditions.

[*Liu et al.,* 2012; *Wegmann et al.,* 2015]. Although in principle modeling studies can isolate the impacts of sea ice and snow, few studies to date have used a fully stratosphere-resolving (i.e., high-top) model and explicitly examined the role of the stratosphere in the Arctic-midlatitude climate linkage [e.g., *Fletcher et al.,* 2009]. A recent study based on a high-top model by *Sun et al.* [2015] found that reduced sea ice in the Arctic would lead to significant modulation of the AO behavior and consequential impacts on the surface climate through stratospheric wave mean flow interactions. However, their focus was on a projected sea ice response in a centennial time scale, and there has been no modeling study examining impacts of an observed rapid Arctic sea ice loss with an attention on stratospheric processes using a high-top model. Nor is there a model study directly investigating the role of stratospheric wave mean flow interactions in the context of the sea ice impacts on midlatitudes climate.

Here we show that based on numerical experiments using a high-top atmospheric general circulation model [*Nakamura et al.,* 2015] that has already shown sea ice impacts on the stratosphere highly consistent with observations, midlatitude surface signals as a response to the Arctic sea ice reduction disappear when artificially suppressing stratospheric wave mean flow interaction. The results confirm the active role of the stratosphere in the Arctic midlatitude climate linkage. Then, from a posteriori analysis we argue that an observed reduction in sea ice alone can sufficiently affect atmospheric circulation to influence surface climate via the stratospheric pathway.

2. Methods

2.1. Data

The Merged Hadley-National Oceanic and Atmospheric Administration/Optimum Interpolation sea surface temperature (SST) and sea ice concentration (SIC) data sets [*Hurrell et al.,* 2008] for the period 1979–2011 were used for the boundary conditions of the model. The model simulated turbulent heat fluxes over ice-covered and open-water grid cells in the Arctic Ocean were comparable to observation-based fluxes. To demonstrate the influence of actual sea ice reductions during recent decades, we defined *Early* (5 year average of 1979–1983) and *Late* (2005–2009) periods, when the ice cover was heavy and light, respectively. The calculated change in sea ice (*Late* minus *Early*) showed large sea ice reductions in the East Siberian Sea in summer, the Barents-Kara Sea and Bering Strait in winter, and the Okhotsk Sea in late winter [see *Nakamura et al.*, 2015, Figure 1].

2.2. Model and Experimental Design

We used the atmospheric general circulation model for the Earth simulator (AFES) version 4.1 with triangular truncation at horizontal wave number 79 (T79; horizontal resolution approximately 1.5°), 56 vertical levels, and the model top at about 60 km. We performed three sensitivity experiments (*FREE*, *RS10*, and *RS30*), each consisting of two perpetual model runs (high sea ice (*HICE*) and low sea ice (*LICE*)) using sea ice conditions of the *Early* or *Late* periods as summarized in Table 1.

The *FREE* experiment was the same as the sensitivity experiment performed in our previous study [*Nakamura et al.,* 2015], in which sea ice conditions during the *Early* and *Late* periods were used as the boundary conditions for high sea ice (*HICE*) and low sea ice (*LICE*) runs, respectively. Boundary conditions of sea surface temperature (SST) were identical, and the other external forcings were fixed as follows: 380 ppmv for CO_2, 1.8 ppmv for CH_4, and the monthly climatological mean O_3 for 1979–2011, obtained from the Japanese 25 year Reanalysis/Japan Meteorological Agency Climate Data Assimilation System reanalysis data. Default

values of aerosol and incident solar radiation were used. More detailed description of the experimental settings can be found in our previous paper [*Nakamura et al.,* 2015]. Using the 60 year output of the two runs, which followed an 11 year spin-up, we examined the atmospheric responses to differences in the sea ice conditions.

The *RS10* experiment differed from *FREE* in that the zonal mean zonal wind above 10 hPa was restored at every time step by relaxation toward the climatology of the daily annual cycle in the *HICE* run of *FREE* with a maximum relaxation timescale of 1 day. Relaxation forcing τ^{-1} was zero ($\tau = \infty$) at and below the lowest level of 10 hPa and increased linearly up to 1.0 d^{-1} ($\tau = 1$ day) at the higher level of 3.16 hPa, and was 1.0 d^{-1} above that level. The *RS30* experiment was the same as *RS10* except that the lowest level was 31.6 hPa and the higher level was 10 hPa (Text S1 in the supporting information). Because our experiments restored the zonal mean component of the zonal wind but not the eddy (departure from the zonal mean) component, interaction of the planetary wave and the mean flow was suppressed by damping feedback from the wave to the mean flow rather than by damping the amplitude of the wave itself. By this suppression of wave mean flow interaction, *RS10* and *RS30* partially emulated the low-top models, which are often used for climate simulations (e.g., phase 3 of the Coupled Model Intercomparison Project). It should be noted that the restoring force leads small biases in the climatological state (discussed in supporting information Text S2). As an additional check on possible changes in the dominant circulation pattern in the troposphere during our restoring experiments, we examined the first empirical orthogonal function in the Northern Hemisphere troposphere in all experiments and confirmed that the AO pattern was the first dominant mode in all experiments.

2.3. Statistics and Techniques

In the individual experiments, we examined the differences in the 60 year averages of *LICE* minus *HICE*, in which only the sea ice difference was responsible for the atmospheric anomalies. Statistical significance was examined by a two-tailed standard *t* test for pairs of the 60 samples. Transformed Eulerian mean diagnostics were used to determine the vertical component of the Eliassen-Palm (E-P) flux (F_z), an indicator of the upward propagation of planetary-wave activity. The 5 day running means of zonal mean zonal wind and F_z were used for daily temporal anomalies. The polar cap height (PCH) was defined as geopotential height averaged northward of 65°N at each pressure level. Variations of the daily mean PCH during the 90 days of winter (December–February) were used to diagnose the vertical coupling intensity in the three experiments. Eddy geopotential heights were defined as departures of the geopotential height from its zonal mean. The three-dimensional E-P flux [*Plumb,* 1985] was used to diagnose the three-dimensional structure of wave activity in the model.

3. Results

3.1. Different Sea Ice Impacts Due To Representation of the Stratosphere

We evaluated the simulated responses to sea ice reduction in the Arctic region by subtracting the *HICE* results from the *LICE* results. Hereafter, we refer to these differences as anomalies. In the *FREE* experiment, the geopotential height anomalies in the upper troposphere at 300 hPa averaged over December–February clearly showed the negative AO phase pattern, which is characterized by positive anomalies over the Arctic and negative anomalies in surrounding regions (Figure 1b). At 2 m height, large negative (cold) air temperature anomalies were found over eastern Siberia, and less significant negative anomalies were seen over the Europe and northeastern North America region (Figure 1c). These results are highly consistent with observations that following a low summertime sea ice cover in the Arctic, the wintertime AO tends to be in its negative phase, which brings severe winter weather to Eurasia and the North Atlantic sector [*Francis and Vavrus,* 2012; *Barnes,* 2013; *Cohen et al.,* 2014; *Screen and Simmonds,* 2014; *Kim et al.,* 2014; *Nakamura et al.,* 2015; *Sun et al.,* 2015]. In the stratosphere the signal of the negative AO phase was marked in the geopotential height anomalies at 50 hPa (Figure 1a).

When restoration was applied, the stratospheric AO signal was not so different (*RS10*) or was slightly weakened (*RS30*). In contrast, no clear AO signal at 300 hPa (Figure 1b) nor any significant cold anomalies (Figure 1c) was seen in eastern Siberia. Instead, a significant cold anomaly was seen over northwestern North America only in *RS10*. These results show that by damping stratospheric variations, the tropospheric

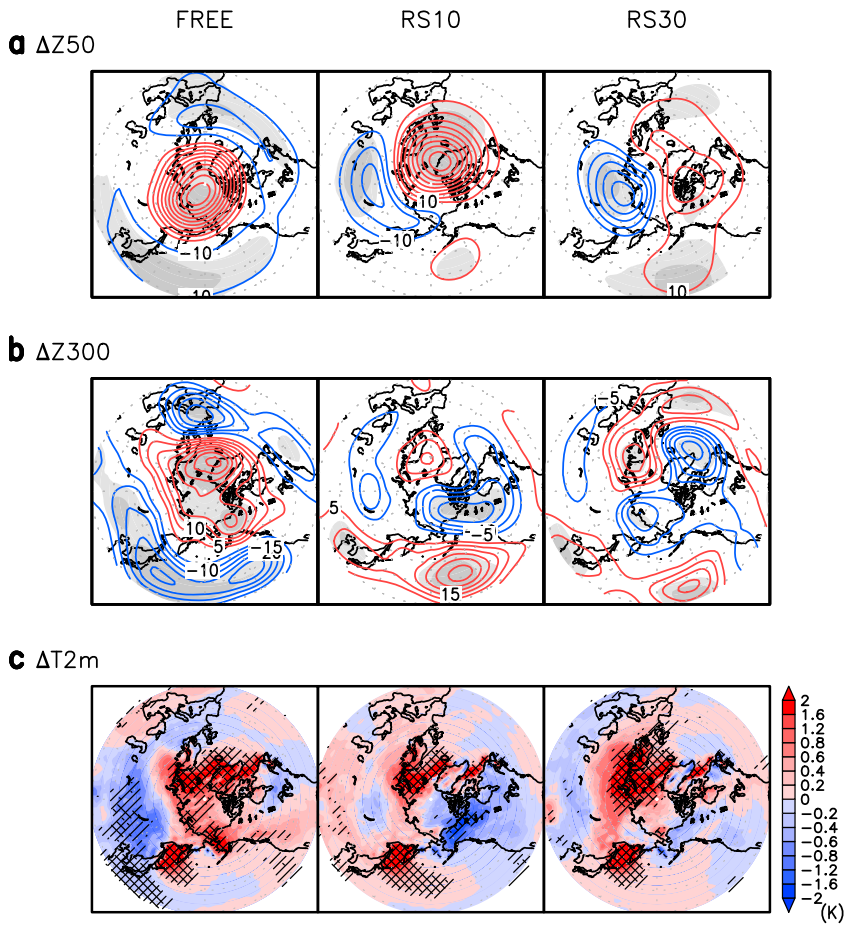

Figure 1. December–February averaged anomalies (*LICE* minus *HICE*) of (a) geopotential height at 50 hPa (in m); (b) geopotential height at 300 hPa (m); and (c) temperature at 2 m height (K) in the (from left to right) *FREE*, *RS10*, and *RS30* experiments. *LICE* and *HICE* runs indicate perpetual model simulations with annual cycle of low (2005–2009) and high (1979–1983) sea ice conditions, respectively (see section 2). In Figures 1a and 1b, red (blue) contours indicate amplitudes of the positive (negative) anomaly, with the zero line omitted. Light and heavy grey shades indicate statistical significance greater than 95% and 99%, respectively. In Figure 1c, red (blue) shading indicates positive (negative) anomalies. Hatching (cross hatching) indicates statistical significance greater than 95% (99%).

response to the sea ice reduction was modified in such a way that the negative AO-like pattern and its associated cold anomalies in the troposphere were much subdued or even absent in the experiments with restored stratospheric circulation. Furthermore, the surface temperature anomalies differ among three experiments except for warm anomalies over ice reduction regions, suggesting large natural fluctuations of the temperature responses that hinder to detect sea ice impacts on the surface [*Mori et al.,* 2014].

3.2. Dynamical Processes

Central to stratosphere-troposphere coupling is a dynamical process by which planetary-scale waves propagate upward, followed by weakening of the stratospheric polar vortex and the downward progress of its signal back to the troposphere [*Baldwin and Dunkerton,* 2001; *Nishii et al.,* 2011; *Kidston et al.,* 2015]. These components were all clearly identified as responses to sea ice reduction in the *FREE* experiment. During December–March, an increase in anomalies in the vertical component of the Eliassen-Palm (E-P) flux (F_z) at 100 hPa averaged over the 50–80°N latitude band (a measure of the upward propagation of planetary-scale wave activity) just prior to a period of negative anomalies in the zonal mean zonal winds at 60°N in the upper stratosphere was followed 1 to 3 weeks later by downward propagation of the stratospheric signal to the troposphere (Figures 2a and 2b). These temporal characteristics were further captured by a lead-lag correlation map of polar cap height (PCH) anomalies (Figure 2c). From the reference height of 100 hPa, the upper

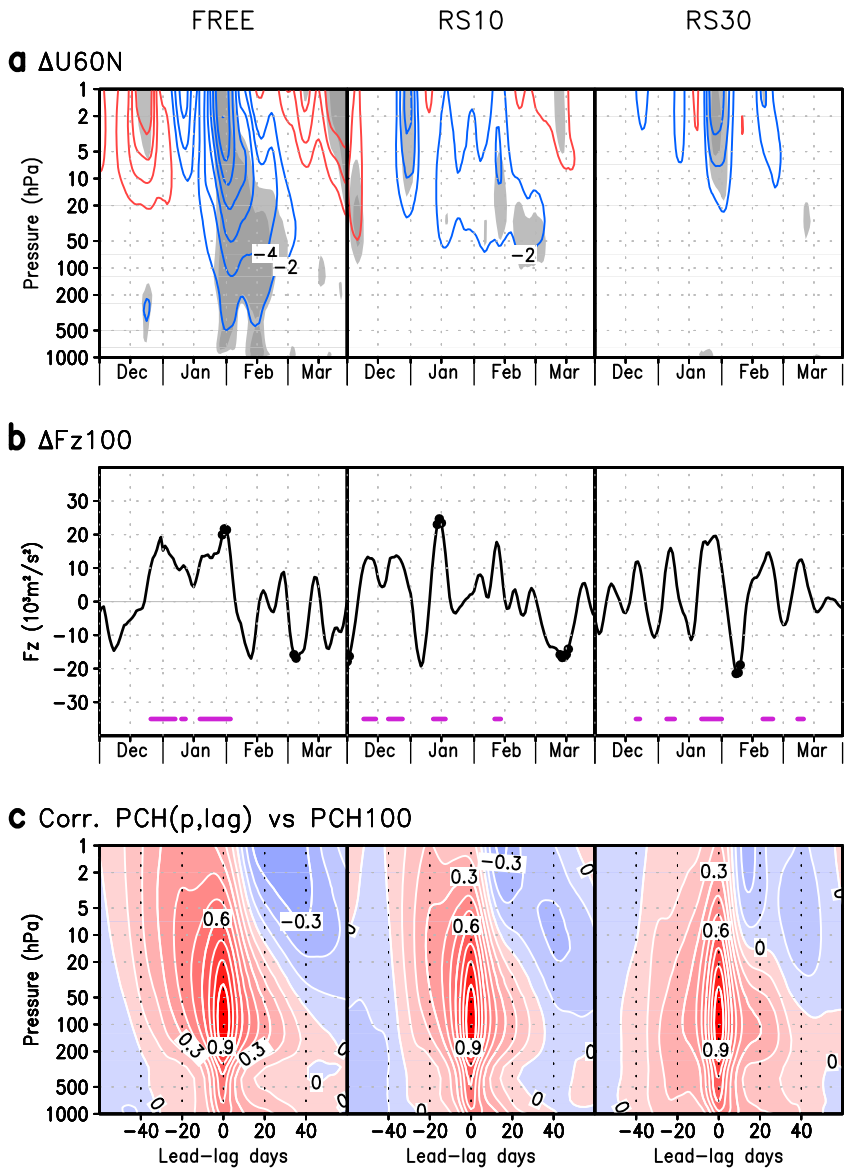

Figure 2. (a) Time-height cross sections of daily mean anomalies (*LICE* minus *HICE*) of zonal mean zonal wind at 60°N. Red (blue) contours indicate amplitudes of the positive (negative) anomaly, with the zero line omitted. Light and heavy grey shades indicate statistical significance greater than 95% and 99%, respectively; the contour interval is 2.0 m s^{-1}. (b) Time series of daily anomalies of F_z (vertical component of the Eliassen-Palm flux) at 100 hPa averaged over 50–80°N. Black dot indicates the statistical significance greater than 95%. Purple line segments signify periods when the F_z anomaly exceeded 10^4 m^2 s^{-2}. (c) Lead-lag correlation coefficients of polar cap height (PCH) at various pressure levels with PCH at 100 hPa. Red (blue) shading indicates positive (negative) correlations; contour interval is 0.1.

stratosphere PCH anomalies led by up to 2 weeks, and the tropospheric PCH anomalies lagged on a much shorter timescale; together they indicate slow downward propagation of the stratospheric signal and faster coupling between the lower stratosphere and the troposphere.

These signatures were much reduced in *RS10*. Although similar negative wind anomalies in the stratosphere appeared after some intensification of upward wave propagation in December and January, their amplitudes were smaller, and the signal was less significant compared with the signatures in *FREE*. Importantly, the signal no longer reached the troposphere (Figures 2a and 2b). In *RS30*, there was no significant downward propagation of the stratospheric signal (Figure 2a). One might think that the stratosphere-troposphere coupling would be weak in the restored experiments. On the contrary, at zero lag stratosphere-troposphere coupling was seen in all three experiments (Figure 2c). Thus, one of the reasons for the lack of a tropospheric signal in

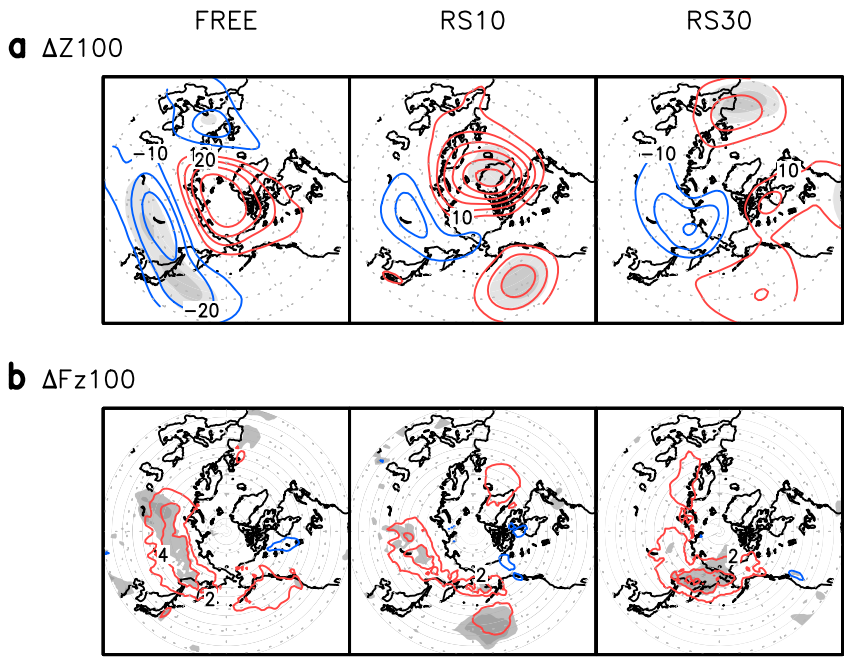

Figure 3. January *LICE*-minus-*HICE* anomalies of (a) geopotential height at 100 hPa (m) and (b) vertical component of the wave activity flux at 100 hPa (10^3 m^2 s^{-2}). Contours indicate amplitudes of the anomaly with the zero line omitted. Light and heavy grey shadings indicate statistical significance over 95% and 99%, respectively.

RS10 is that the signal in the lower stratosphere was too weak; this was caused by the unrealistically weak amplitudes of the anomalies in the upper stratosphere (supporting information Figure S1b), which therefore no longer propagated to the lower stratosphere. The fact that the lead-lag structure in the upper stratosphere was degraded in a stepwise manner with restoration (Figure 2c) provides strong evidence for an active stratospheric dynamic role and at the same time suggests the importance of the upper stratosphere.

To strengthen our case for the critical role of the stratosphere, we examined the details of upward propagation of planetary-scale waves. We note that anomalous upward propagation of planetary-scale waves occurred mainly over eastern Siberia (Figure 3b) in all three experiments. The colocation of these anomalies with geopotential height anomalies and their respective climatological locations (Figure 3a and supporting information Text S3) indicated that the deepening of the climatological trough over eastern Siberia is key to the anomalous upward propagation of planetary-scale waves. This robustness of the spatial distribution of the upward propagation across the experiments is expected because restoring the zonal winds did not suppress the amplitude of the waves; it only suppressed the interaction of the waves with the mean flow. The upward E-P flux anomaly in January was persistently positive in *FREE* (purple lines in Figure 2b), reflecting more frequent occurrence of upward propagating wave packet with longer duration. This suggests the presence of some two-way interactions in which planetary-wave modulation is affected by the stratosphere-troposphere coupling process itself (discussed in supporting information Text S4). That is, the anomalous upward wave propagation is not only induced by the tropospheric wave source but also intensified by the stratospheric circulation changes, as has been suggested previously [*Harnik,* 2009; *Nishii et al.,* 2011].

3.3. Possible Snow Cover Influences

Finally, we examined the possibility that snow cover changes induced by sea ice changes could have triggered stratospheric processes. The correlation between the snow-covered area in Siberia (see supporting information Text S5 for details) and the strength of the tropospheric AO was negative ($r = -0.25$; $p = 0.054$) in the *HICE* run of the *FREE* experiment. This result may be taken as evidence for snow cover impacts on the surface climate in winter [*Fletcher et al.,* 2007, 2009; *Peings et al.,* 2012]. However, we found no appreciable difference in the snow cover extent between the *HICE* and *LICE* runs in the *FREE* experiment. On the basis of this a posteriori analysis we argue that changes in sea ice conditions alone have a sufficiently large and direct

influence on atmospheric circulation and onto surface climate via the stratospheric pathway, without invoking indirect impacts from the induced snow cover changes.

4. Discussion and Concluding Remarks

It is a challenging task to fully understand the Arctic midlatitudes climate linkage, especially the AO phase as a response to changing Arctic climate. Atmospheric circulation responses to sea ice anomalies vary among different models and experiments, and both positive and negative AO-like responses to the Arctic sea ice changes have been reported [e.g., *Screen and Simmonds,* 2014; *Barnes and Screen*, 2015; *Sun et al.*, 2015]. The responses vary depending on an exact period and a region of sea ice anomalies in question (see the discussion in *Sun et al.* [2015]). In this context, it is worth stating that our simulation was based on sea ice anomalies representing rapid changes over the last three decades with the strongest influence from the late-fall turbulent heat flux anomalies in the Barents-Kara Seas as discussed in *Nakamura et al.* [2015]. Within this framework, our results suggest that the observed Arctic sea ice variations, by triggering stratospheric processes, have potential to exert significant weather and climate influences on the Northern Hemisphere midlatitudes. For better understanding of the Arctic midlatitudes climate linkage, a comparison with observations in terms of magnitudes of signals with a careful analysis on combined impacts from different sources and pathways are clearly needed in future. In particular, large part of the differences among the previous results can be traced to a different basic state of the stratosphere and/or a particular phase of the responses relative to climatological stationary-wave structure [*Smith et al.,* 2010; *Nishii et al.,* 2011], which will be covered in our future work.

The present results indicate climate models, which contain the whole stratosphere, are indispensable for realistic climate predictions. The stratosphere now appears to be influenced by various sources. Our results place Arctic sea ice in an already long list of forcings, including tropical sea surface temperature (e.g., El Niño–Southern Oscillation), ozone, and greenhouse gases, that can affect the stratospheric polar vortex strength with consequential downward influences on the surface climate [*Brönnimann et al.,* 2004; *Manzini et al.,* 2006; *Ineson and Scaife,* 2009; *Kidston et al.,* 2015]. For better climate predictions, besides a deeper understanding of stratosphere-troposphere coupling mechanisms, there is an urgent need to understand the combined influences of these various sources on the stratosphere.

Acknowledgments
We thank K. Dethloff, D. Handorf, and R. Jaiser for helpful discussions and comments. Merged Hadley-NOAA/OI SST and SIC data were obtained from the Climate Data Guide provided by the National Center for Atmospheric Research (NCAR) and University Corporation for Atmospheric Research (UCAR) (https://climatedataguide.ucar.edu/). The AFES simulations were performed on the Earth simulator at the Japan Agency for Marine-Earth Science and Technology (JAMSTEC). To access our AFES simulation data, contact the corresponding author (nakamura.tetsu@ees.hokudai.ac.jp). This study was supported by the Green Network of Excellence Program (GRENE Program) Arctic Climate Change Research Project and the Japanese Ministry of Education, Culture, Sports, Science and Technology (MEXT) through a Grant-in-Aid for Scientific Research in Innovative Areas 2205. The authors have no competing interests that might be perceived to influence the results and/or discussion reported in this article.

References

Baldwin, M. P., and T. J. Dunkerton (2001), Stratospheric harbingers of anomalous weather regimes, *Science*, *294*, 581–584.
Barnes, E. A. (2013), Revisiting the evidence linking Arctic amplification to extreme weather in midlatitudes, *Geophys. Res. Lett.*, *40*, 1–6, doi:10.1002/grl.50880.
Barnes, E. A., and J. A. Screen (2015), The impact of Arctic warming on the midlatitude jetstream: Can it? Has it? Will it?, *WIREs Clim. Change*, *6*, 277–286.
Barriopedro, D., and R. Garcia-Herrera (2006), A climatology of Northern Hemisphere blocking, *J. Clim.*, *19*, 1042–1063, doi:10.1175/JCLI3678.1.
Brönnimann, S., J. Luterbacher, J. Staehelin, T. M. Svendby, G. Hansen, and T. Svenøe (2004), Extreme climate of the global troposphere and stratosphere in 1940–42 related to El Niño, *Nature*, *431*, 971–974.
Cai, D., M. Dameris, H. Garny, and T. Runde (2012), Implications of all season Arctic sea-ice anomalies on the stratosphere, *Atmos. Chem. Phys.*, *12*, 11,819–11,831.
Cohen, J., et al. (2014), Recent Arctic amplification and extreme mid-latitude weather, *Nat. Geosci.*, *7*, 627–637.
Deser, C., R. Tomas, M. Alexander, and D. Lawrence (2010), The seasonal atmospheric response to projected Arctic sea ice loss in the late 21st century, *J. Clim.*, *23*, 333–351.
Fletcher, C. G., P. J. Kushner, and J. Cohen (2007), Stratospheric control of the extratropical circulation response to surface forcing, *Geophys. Res. Lett.*, *34*, L21802, doi:10.1029/2007GL031626.
Fletcher, C. G., S. C. Hardiman, P. J. Kushner, and J. Cohen (2009), The dynamical response to snow cover perturbations in a large ensemble of atmospheric GCM integrations, *J. Clim.*, *22*, 1208–1222.
Francis, J. A., and S. J. Vavrus (2012), Evidence linking Arctic amplification to extreme weather in mid-latitudes, *Geophys. Res. Lett.*, *39*, L06801, doi:10.1029/2007GL031626.
Harnik, N. (2009), Observed stratospheric downward reflection and its relation to upward pulses of wave activity, *J. Geophys. Res.*, *114*, D08120, doi:10.1029/2008JD010493.
Honda, M., J. Inoue, and S. Yamane (2009), Influence of low Arctic sea-ice minima on anomalously cold Eurasian winters, *Geophys. Res. Lett.*, *36*, L08707, doi:10.1029/2008GL037079.
Hopsch, S., J. Cohen, and K. Dethloff (2012), Analysis of a link between fall Arctic sea ice concentration and atmospheric patterns in the following winter, *Tellus A*, *64*, 18,624.
Hurrell, J. W., J. J. Hack, D. Shea, J. M. Caron, and J. A. Rosinski (2008), A new sea surface temperature and sea ice boundary dataset for the Community Atmosphere Model, *J. Clim.*, *21*, 5145–5153.
Ineson, S., and A. A. Scaife (2009), The role of the stratosphere in the European climate response to El Niño, *Nat. Geosci.*, *2*, 32–36.
Jaiser, R., K. Dethloff, D. Handorf, A. Rinke, and J. Cohen (2012), Impact of sea ice cover changes on the Northern Hemisphere atmospheric winter circulation, *Tellus A*, *64*, 11,595.

Kidston, J., A. A. Scaife, C. Hardiman, D. M. Mitchell, N. Butchart, M. P. Baldwin, and L. J. Gray (2015), Stratospheric influence on tropospheric jet streams, storm tracks and surface weather, *Nat. Geosci.*, *8*, 433–440.

Kim, B. M., S. W. Son, S. K. Min, J. H. Jeong, S. J. Kim, Z. Zhang, T. Shim, and J. H. Yoon (2014), Weakening of the stratospheric polar vortex by Arctic sea-ice loss, *Nat. Commun.*, *5*, 4646.

King, M. P., M. Hell, and N. Keenlyside (2015), Investigation of the atmospheric mechanisms related to the autumn sea ice and winter circulation link in the Northern Hemisphere, *Clim. Dyn.*, doi:10.1007/s00382-015-2639-5.

Liu, J. P., J. A. Curry, H. Wang, M. Song, and R. M. Horton (2012), Impact of declining Arctic sea ice on winter snowfall, *Proc. Natl. Acad. Sci. U.S.A.*, *109*, 4074–4079.

Manzini, E., M. A. Giorgetta, M. Esch, L. Kornblueh, and E. Roeckner (2006), The influence of sea surface temperatures on the northern winter stratosphere: Ensemble simulations with the MAECHAM5 Model, *J. Clim.*, *19*, 3863–3881.

Mori, M., M. Watanabe, H. Shiogama, J. Inoue, and M. Kimoto (2014), Robust Arctic sea-ice influence on the frequent Eurasian cold winters in past decades, *Nat. Geosci.*, *7*, 869–873.

Nakamura, T., K. Yamazaki, K. Iwamoto, M. Honda, Y. Miyoshi, Y. Ogawa, and J. Ukita (2015), A negative phase shift of the winter AO/NAO due to the recent Arctic sea-ice reduction in late autumn, *J. Geophys. Res. Atmos.*, *120*, 3209–3227, doi:10.1002/2014JD022848.

Nishii, K., H. Nakamura, and Y. J. Orsolini (2011), Geographical dependence observed in blocking high influence on the stratospheric variability through enhancement or suppression of upward planetary-wave propagation, *J. Clim.*, *24*, 6408–6423.

Orsolini, Y. J., R. Senan, R. E. Benestad, and A. Melsom (2012), Autumn atmospheric response to the 2007 low Arctic sea ice extent in coupled ocean–atmosphere hindcasts, *Clim. Dyn.*, *38*, 2437–2448, doi:10.1007/s00382-011-1169-z.

Overland, J., K. Wood, and M. Wang (2011), Warm Arctic-cold continents: Climate impacts of the newly open Arctic Sea, *Polar Res.*, *30*, 15,787.

Peings, Y., D. Saint-Martin, and H. Douville (2012), A numerical sensitivity study of the influence of Siberian snow on the Northern Annular Mode, *J. Clim.*, *25*, 592–607.

Plumb, R. A. (1985), On the three-dimensional propagation of stationary waves, *J. Clim.*, *42*, 217–229.

Screen, J. A., and I. Simmonds (2014), Amplified mid-latitude planetary waves favour particular regional weather extremes, *Nat. Clim. Change*, *4*, 704–709.

Smith, K. L., C. G. Fletcher, and P. J. Kushner (2010), The role of linear interference in the Annular Mode response to extratropical surface forcing, *J. Clim.*, *23*, 6036–6050.

Sun, L., C. Deser, and R. A. Tomas (2015), Mechanisms of stratospheric and tropospheric circulation response to projected Arctic sea ice loss, *J. Clim.*, *28*, 7824–7845.

Thompson, D. W. J., and J. M. Wallace (1998), The Arctic Oscillation signature in the wintertime geopotential height and temperature fields, *Geophys. Res. Lett.*, *25*, 1297–1300, doi:10.1029/98GL00950.

Thompson, D. W. J., and J. M. Wallace (2001), Regional climate impacts of the Northern Hemisphere Annular Mode, *Science*, *293*, 85–89.

Vavrus, S., J. E. Walsh, W. L. Chapman, and D. Protis (2006), The behavior of extreme cold air outbreaks under greenhouse warming, *Int. J. Climatol.*, *26*, 1133–1147, doi:10.1002/joc.1301.

Wegmann, M., Y. Orsolini, M. Vázquez, L. Gimeno, R. Nieto, O. Bulygina, R. Jaiser, D. Handorf, A. Rinke, and K. Dethloff (2015), Arctic moisture source for Eurasian snow cover variations in autumn, *Environ. Res. Lett.*, *10*, 054015.